This paper is published in Plant and Cell Physiology (2017) 58 (4), 760-769.
doi:10.1093/pcp/pcx008

SRPP, a cell-wall protein is involved in development and protection of seeds and root hairs in *Arabidopsis thaliana*

Running head: A cell-wall protein protects seeds and root hairs

Natsuki Tanaka[1], Hiroshi Uno[1], Shohei Okuda[1], Shizuka Gunji[2], Ali Ferjani[2], Takashi Aoyama[3], and Masayoshi Maeshima[1,*]

[1] Laboratory of Cell Dynamics, Graduate School of Bioagricultural Sciences, Nagoya University, Nagoya 464-8601, Japan
[2] Department of Biology, Tokyo Gakugei University, Nukui Kitamachi 4-1-1, Koganei-shi, Tokyo 184-8501, Japan
[3] Institute for Chemical Research, Kyoto University, Gokasho, Uji, Kyoto 611-0011, Japan
*Corresponding author: Masayoshi Maeshima, E-mail, maeshima@agr.nagoya-u.ac.jp

Abbreviations: CLSM, confocal laser-scanning microscopy; GFP, green fluorescent protein; GUS, β-glucuronidase; NR23, no root hair line that expresses the N-terminal region (23 residues) of PCaP2; PI, propidium iodide; PRP, proline-rich protein; SEM, scanning electron microscopy; SRPP, seed and root hair protective protein; TEM, transmission electron microscopy.

Abstract

Enhancement of root hair development in response to phosphate (Pi) deficit has been reported extensively. Root hairs are involved in major root functions such as the absorption of water, acquisition of nutrients, and secretion of organic acids and enzymes. Individual root hair cells maintain these functions and appropriate structure under various physiological conditions. We examined to identify protein(s), which keep the structure and function of root hairs, and identified a protein (SEED AND ROOT HAIR PROTECTIVE PROTEIN, SRPP) that was induced in root hairs under Pi deficient conditions. Promoter assay and mRNA quantification revealed that SRPP was expressed in root hairs and seeds. A knockout mutant, *srpp-1*, consistently displayed defects in root hairs and seeds. Root hairs in *srpp-1* were short and the phenotypes observed under Pi-deficient conditions were also detected in ethylene-treated *srpp-1* plants. Propidium iodide stained most root hairs of *srpp-1* grown under Pi-deficient conditions, suggesting cell death. In addition to root hairs, most *srpp-1* seeds were withered and their embryos were dead. SRPP tagged with green fluorescent protein was detected in the cell wall. Electron microscopy showed abnormal morphology of the cell wall. Wild-type phenotypes were restored when the *SRPP* gene was expressed in *srpp-1*. These data strongly suggest that *SRPP* contributes to the construction of robust cell walls, whereby it plays a key role in the development of root hairs and seeds.

Keywords: *Arabidopsis thaliana*・Root hair・Seed・Phosphate deficiency・Cell wall

Introduction

In plants, root hairs provide a large surface area that is exposed to the external environment. Root hairs are involved in major root functions, such as absorption of water, acquisition of nutrients, secretion of organic acids and enzymes, interactions with microbes, and providing a physical support for penetration of roots into soil (Gilroy and Jones 2000, Emons and Ketelaar 2009, Libault et al. 2010, Datta et al. 2011, Tanaka et al. 2014). Root hair surfaces are exposed to soil and are therefore susceptible to biotic and abiotic stresses. Molecular biological studies on the differentiation and tip growth of root hairs have developed rapidly and have provided a plethora of information on several key genes and their respective regulatory pathways (Datta et al. 2011, Grebe 2012, Kwasniewski et al. 2013, Grierson et al. 2014). However, there is little information on how root hairs maintain their form and physiological functions against the various biotic and abiotic stresses. Pi deficit enhances root hair development remarkably. These emergently elongating root hairs may provide good materials for understanding maintenance mechanism of the structure and functions. The root hairs maintain both properties of strong structure and nutrient absorption ability of their cell walls. Therefore, we investigated proteins induced in root hairs under Pi deficient conditions.

Previously, we investigated the physiological roles of root hairs by comparing wild-type plants and the root hair-less line, NR23, and also conducted proteomic analyses of roots from NR23 (Tanaka et al. 2014). The transgenic line NR23 expresses a 23-amino acid peptide of the N-terminal region of plasma membrane associated cation-binding protein-2 (PCaP2) (Ide et al. 2007, Kato et al. 2010, 2013) under the control of the root hair-specific *EXPANSIN A7* promoter. NR23 produces no root hairs under any conditions on any part of the roots (Tanaka et al. 2014), due to the inhibition of root hair elongation by the small peptide (Kato et al. 2013). In addition to the differences in the proteomic profiles between wild-type and NR23 plants under normal conditions, we further compared their composition under phosphate (Pi)-deficient conditions and found a particular protein that was increased only in the wild-type roots. The gene encoding this protein was believed to be root hair-specific, based on microarray analysis using another root hair-less mutant, so it was given the name *RHS13* (*Root Hair Specific 13*) (Won et al. 2009). In this study, the expression

of *RHS13* was confirmed in root hairs, but detected also in seeds and other tissues. Therefore, we renamed it SRPP (Seed and Root hair Protective Protein) as explained below.

Here, we found that SRPP is expressed in seeds and root hairs. Mature seeds with tough seed coats are tolerant to harsh conditions such as drought (Haughn and Chaudhury 2005, Rajjou and Debeaujon 2008). Maturing seeds might acquire stress tolerance at an early stage of seed formation in the siliques. Considering the tissue-specific expression and stress tolerance of the above tissues, we focused our attention on the physiological role of SRPP and investigated the phenotypic properties of root hairs and seeds using a transposon-tagged knockout mutant, *srpp-1*. *srpp-1* exhibited short and abnormally shaped root hairs and withered seeds. Furthermore, both root hairs and seeds of the mutant showed a tendency to necrotize. Electron microscopy of *srpp-1* embryos showed thicker cell walls with abnormal structure. When SRPP tagged with green fluorescent protein (GFP) was expressed under its own promoter, the fluorescence was detected clearly in the cell walls. Thus we describe the uniqueness of SRPP among other cell wall proteins such as proline (Pro)-rich protein (PRP), and discuss its physiological role in the cell wall.

Results

Identification of SRPP in roots grown under Pi-deficient conditions

The root-hair less NR23 line provides valuable information for identification of root-hair specific components by comparison with the wild-type roots, because NR23 line forms no root hair under any conditions in any regions of the roots. We performed proteomic analysis of the crude membrane fractions from the roots of the NR23 line (Tanaka et al. 2014, Kato et al. 2013). Proteomic profiles of Col-0 and NR23 grown under standard and Pi-deficient conditions were compared. A protein with 165 residues, SRPP, was identified only in Col-0 under Pi-deficient conditions (Supplementary Fig. S1). The gene encoding this protein, *RHS13*, has been reported as a root hair-specific gene from the results of the microarray analysis (Won et al. 2009). This study revealed that the RHS13/SRPP protein is present in root hairs and was increased markedly under Pi-deficient conditions. We also confirmed the

induction of transcriptional level of *SRPP* by Pi-deficiency (Supplementary Fig. S2A). *SRPP* transcripts were increased about three times in No-0 under Pi-deficient conditions. Furthermore, we expressed a construct containing *SRPP* linked with GFP under the control of its own promoter. We observed roots of the T_2 generation by confocal laser-scanning microscopy (CLSM) and detected GFP fluorescence in root hairs only under Pi-deficient conditions (Supplementary Fig. S2B – D). This observation is consistent with the results of the proteomic analysis, and suggests that SRPP may play a critical role under Pi deficiency.

***SRPP* is expressed in root hairs, anthers, and fruits**

SRPP transcripts were detected clearly in roots and faintly in siliques of wild-type plants (Fig. 1A). We further investigated the tissue specificity of *SRPP* expression using promoter::GUS analysis. GUS activity was detected in roots but not in shoots grown under normal conditions (Fig. 1B, left; C). In particular, root tips and elongating regions of the primary and lateral roots showed high GUS activity. A magnified view revealed high expression in root hairs and collet hairs (Fig. 1D). Furthermore, plants cultivated under Pi-deficient conditions seemed to have higher GUS activity in roots (Fig. 1B, right).

Next, examination of reproductive organs revealed GUS activity in fruits and anthers (Fig. 1E–G; Supplementary Fig. S3). The GUS activity was detected in the pericarps and receptacles during maturation of siliques (Fig. 1E). Then we stained fruits, from which pericarps were removed, and detected significant activity in the embryo, funiculus, and seed coat in siliques (Fig. 1F). For the embryonic stage, the GUS signal was detected from the initial globular to mature stages (Fig. 1F, G). In seed coats, the signal was detected in the transparent inner integument (Fig. 1G). We also detected the GUS activity in anthers, whereby the GUS signal in young anthers was stronger than in mature ones (Supplementary Fig. S3).

No detection of SRPP protein or green fluorescence of SRPP-GFP in plants grown under normal conditions is inconsistent with the observations of mRNA quantification and promoter::GUS analysis. This may be due to slow translation rate and/or rapid degradation of SRPP under normal condition.

Growth of *srpp-1* under normal conditions

We characterized an *SRPP* loss-of-function mutant to investigate the physiological roles of SRPP. The *srpp-1* mutant line of *Arabidopsis thaliana* (strain Nossen-0, No-0) has a transposon insertion in the first exon of *SRPP* (Supplementary Fig. S4A). We used *srpp-1* as a functionally defective mutant of SRPP, because no *SRPP* transcripts were detected in this mutant plants (Fig. 1A, Supplementary Fig. S2A). The mutant *srpp-1* grew normally and there was no difference in the primary root length or shoot fresh weight between No-0 and *srpp-1* (Supplementary Fig. S4B, C). Also, the *srpp-1* mutant grown under normal conditions showed no difference in the root hair length compared to No-0 (Fig. 2A).

Root hair elongation in *srpp-1* under Pi-deficient conditions is attenuated

In contrast to results found under normal conditions, the length of primary roots of *srpp-1* was 27% shorter than that of No-0 when grown under Pi-deficient conditions for 28 d (Fig. 2B). It is known that the number and length of root hairs in various plants are increased markedly under Pi-deficient conditions (Foehse and Jungk 1983, Gahoonia et al. 2001, Ma et al. 2001). Under Pi-deficient conditions, SRPP expression was increased and detected in root hairs as mentioned above. Thus, we assumed that SRPP is involved in the physiological processes that promote the development and elongation of root hairs.

Then, we compared the length of root hairs of No-0 and *srpp-1* under Pi-deficient conditions. The root hair length reached a maximum at 3 mm from the root tip in both lines (Supplementary Fig. S5). The average length of mature root hairs of No-0 was 0.8 mm. The *srpp-1* root hairs (0.5 mm in length) were 36% shorter than the No-0 root hairs (Fig. 2A). There was no marked difference in the distribution of root hair density (data not shown). In addition to the less pronounced enhancement of root hair elongation in *srpp-1*, bent and drooping root hairs were frequently observed at the upper regions of 15 mm and farther from the root tip (Fig. 2C).

For confirmation, we introduced the *SRPP* gene into the *srpp-1* background under the control of the *SRPP* promoter. In five independent complementation lines, under Pi-deficient conditions, the root hair length, primary root length, and shoot fresh weight, were recovered to the values of No-0 (Supplementary Fig. S6A, C, D). The

number of bent or drooping root hairs in these complementation lines was also decreased (Supplementary Fig. S6B). The results suggest that the phenotypes observed in *srpp-1* under Pi-deficient conditions were caused by the lack of a functional *SRPP* gene.

Phenotype of *srpp-1* after ethylene treatment

The above-mentioned results led us to investigate which physiological elements of Pi-deficient conditions or emergent elongation of root hairs are related directly to the induction and role of SRPP. If SRPP is tightly related to the emergent elongation of root hairs, the phenotype should be observed regardless of Pi availability. Therefore, we attempted to compare the root hairs of No-0 and *srpp-1* plants after ethylene treatment, which is known to enhance the formation and elongation of root hairs (Pitts et al. 1998, Dolan 2001). After ethylene treatment, the length of mature root hairs of *srpp-1* was 29% shorter than root hairs of No-0 (Supplementary Fig. S7A). Furthermore, most root hairs at the upper 15-mm region from the root tip were bent, a phenotype mimicking root hairs grown under Pi-deficient conditions (Supplementary Fig. S7B). These results suggested that SRPP is somehow involved in elongation and maintenance of the structure of root hairs, which are emergently elongated.

***srpp-1* root hairs show necrosis under Pi-deficient conditions**

Roots of No-0 and *srpp-1* were stained with propidium iodide (PI), which is a membrane-impermeable fluorescent dye that is used for cell wall staining and that also allows the distinction between live and dead cells. Roots and root hairs of both No-0 and *srpp-1* were normal under Pi-sufficient conditions, since only cell walls were PI-stained (Fig. 2D). While almost all the root hair cells of *srpp-1* absorbed the dye under Pi-deficient conditions, most of the No-0 root hair cells did not (Fig. 2E). This result indicated that necrosis occurs in root hairs of *srpp-1* under Pi-deficient conditions.

Seeds of *srpp-1* are defective

Careful observation of phenotype during the whole plant life cycle revealed that *srpp-1* seeds are dark brown and withered, even when collected from plants cultivated under

standard conditions (Fig. 3A). To gain further insights, we observed *srpp-1* seeds using a scanning electron microscope (SEM) and found the following phenotypes; (i) the seeds were withered, (ii) the seed surface was hollowed, and (iii) the surface structure of polygonal epidermal cells was altered significantly (Fig. 3B). Then, we removed the seed coats and observed embryos. All embryos of No-0 had a normal shape and almost equal size (the major axis, approximately 0.5 mm). In contrast, embryos of withered *srpp-1* seeds were small and their size was variable (Fig. 3C), while a fraction of *srpp-1* seeds were not withered and their embryos were comparable in size and shape to those of No-0. In addition, cells of embryos were well stained with PI, indicating that most cells of the embryo died in the withered *srpp-1* seeds (Fig. 3D). These results suggest that SRPP is required for normal embryonic development.

Furthermore, the typical phenotypes of *srpp-1* seeds were clearly compensated for by introducing *SRPP*. When No-0, *srpp-1*, and five complementation lines were cultivated side by side under the same conditions, there were no withered seeds in complementation line 1 and 2 (hereinafter referred to as *comp1* and *comp2*; Supplementary Fig. S8). The ratios of withered seeds were less than 10% in *comp3*, *comp4*, and *comp5*. Together, these results indicated that the withered seed phenotype was also due to the lack of *SRPP*.

Functions of SRPP in fruits are predominant in maternal tissues

Seeds are composed of maternal tissues and new tissues made after fertilization. While the seed coat and pericarps are maternal tissues, the embryo is a hybrid tissue. We analyzed characteristics of seeds obtained by crossbreeding No-0 and *srpp-1* to investigate the tissues in which SRPP functions. If a seed phenotype depends directly on its mother (pistil), it means that SRPP plays a very important role in mother tissues and *vice versa*. We crossed No-0 and *srpp-1*, sowed the obtained F_1 seeds, and estimated the germination rate (Fig. 4A). Prior to evaluation, we extracted the genomic DNA from seedlings and confirmed that they were heterozygous for *SRPP*. When No-0 was used as the mother plant for crossing, the average germination rate was 70%. Surprisingly, when *srpp-1* was used as the mother plant, the germination rate was 4% (Fig. 4B). The above results indicated clearly that expression of SRPP in

maternal tissues (pericarps and seed coat) is critical for seed formation. When the mother plant was No-0, the germination rate (70%) was lower than that of No-0, suggesting that SRPP is important for seed formation, even in the hybrid tissue of the embryo.

SRPP is localized in the cell wall

As mentioned above, we expressed SRPP linked with GFP under the control of its own promoter. We observed roots of the T_2 generation by CLSM and detected GFP fluorescence in root hairs (Fig. 5A). Additionally, the SRPP-GFP introduced into *srpp-1* complemented the *srpp-1* phenotypes shown in root hairs and seeds. This indicates that SRPP-GFP expressed in plants shows normal functions (Supplementary Fig. S9A, B). Importantly, the SRPP-GFP signal was detected only under Pi-deficient conditions (Supplementary Fig. S2). The fluorescence was detected in cell walls or plasma membranes (Fig. 5A, B). After plasmolysis, the signal was detected in part of the cell wall, but not in the plasma membrane (Fig. 5C, D). Also, we detected the fluorescence in the cell wall of the basal part (not at the tip) of the root hair at an early stage of elongation (Fig. 5E, F). Although the fluorescence was fairly detected in the root hairs at the bulge-forming stage (Supplementary Fig. S9C), the fluorescence was clearly detected in the basal and middle regions at the elongation stage (Supplementary Fig. S9D, E). Finally, the clear signal was detected through the root hairs including the tips at the mature stage (Supplementary Fig. S9F).

***srpp-1* embryos show structural deformation of the cell wall**

The localization of SRPP to the cell wall led us to examine the structure of the embryo cell wall in withered *srpp-1* seeds by transmission electron microscopy (TEM; Fig. 5G–J). While No-0 embryos had well-balanced polygons (Fig. 5G, I), the cell walls in the *srpp-1* embryos were uneven and the cell shape was distorted (Fig. 5H, J). The cell wall of *srpp-1* was thicker than that of No-0 (Fig. 5K) and the structure of the cell wall was wavy (Fig. 5H, J). The cell wall showed marked hypertrophy especially at the point where three cells meet.

Discussion

The present study of the phenotypic properties of *srpp-1* clarified the importance of SRPP for normal growth of root hairs and seeds. It was revealed that all phenotypes including the abnormal shape of root hairs, shrunken seeds, and the decreased root hair length were restored to normal in five complementation lines (Supplementary Figs. S6, S8). Thus we deduced that these phenotypic aberrations were caused specifically by the loss of functional SRPP.

The primary structure of SRPP is unique among cell wall proteins

In *A. thaliana*, the close paralogous proteins to SRPP are Pro-rich protein 3 (AtPRP3) and Pro-rich protein 1 (AtPRP1) (Supplementary Fig. S10) (BLAST, http://blast.ncbi.nlm.nih.gov/Blast.cgi). However, SRPP lacks a Pro-rich domain in its N-terminal region, which is approximately half the length of AtPRPs (Supplementary Fig. S11). There is 40% identity between SRPP and AtPRPs, excluding the Pro-rich region. SRPP is conserved in various plant species such as *Arabidopsis lyrata* and *Brassica napus*, which have orthologous proteins with 92% and 84% identities, respectively, to SRPP (BLAST). *Theobroma cacao*, *Prunus persica*, *P. mume*, *Glycine max*, *Vitis vinifera*, and *Fragaria vesca* also have orthologous proteins with approximately 40–50% identity to SRPP (Supplementary Fig. S10). SRPP is therefore widely conserved in the plant kingdom, and should have an essential physiological role. SRPP and homologous proteins contain two partially conserved regions (Supplementary Fig. S11). At present it is unclear whether the resemblance in these conserved regions reflects any biochemical role in plants. Each region contains multiple proline and two cysteine residues at the same positions. Biochemical analyses are needed to clarify the potential formation of intra- and inter-molecular disulfide bonds and their functional roles. The highly conserved proline residues might increase the structural flexibility of SRPP and the homologous proteins. Further structural analysis should provide information on the structure-function relationship.

Among paralogs of SRPP, only *A. thaliana* PRP3 (AtPRP3) and PRP-like protein-1 (AtPRPL1) were shown to be expressed in root hairs (Bernhardt and Tierney 2000, Boron et al. 2014). AtPRPL1, which shares 27% identity with SRPP, was shown to be

expressed specifically in root hairs and partially involved in root hair elongation (Boron et al. 2014). SRPP has different characteristics from the above paralogs. For example, the expression of SRPP is induced significantly under Pi-deficient conditions (Supplementary Figs. S1, S2). The *srpp-1* mutant shows an altered phenotype only in elongated root hairs grown under Pi-deficient conditions or when treated with ethylene (Fig. 2; Supplementary Figs. S5, S7). Furthermore, SRPP is expressed not only in the root hair but also in the pericarp, seed, embryo and funiculus (Fig. 1) and is needed both for root hair development and seed formation (Figs. 2, 3). Therefore, SRPP might play a specific role, which is different from that of PRPs and their related proteins.

Cell wall localization of SRPP

The cell wall localization of SRPP was revealed by expression of the GFP-tagged protein in the wild-type (Fig. 5) and *srpp-1* plants (Supplementary Fig. S9D–F). Functionality of SRPP tagged with GFP was evidenced by the result that the expression of SRPP-GFP in *srpp-1* complemented the phenotypes observed in *srpp-1* (Supplementary Fig. S9A, B). In MS analysis, SRPP was identified in the crude membrane fraction prepared from roots (Supplementary Fig. S1), although the protein has no obvious transmembrane domain except for the N-terminal signal sequence. Thus, SRPP is localized in the cell wall space and probably associated with the plasma membrane. SRPP is predicted to have a signal peptide consisting of 24 residues in the N-terminal region (SignalP 4.1; http://www.cbs.dtu.dk/services/SignalP/) (Supplementary Fig. S11) similar to several homologous proteins including AtPRP3, which is thought to be a cell wall protein (Bernhardt and Tierney 2000).

Possible functions of SRPP in root hairs and seeds

The lack of SRPP resulted in shorter root hairs, and eventually led to necrosis under Pi-deficient conditions, but not under normal growth conditions (Fig. 2). We briefly discuss possible physiological functions of SRPP in the cell wall of root hairs. Fluorescence of SRPP-GFP was not detected in the bulge forming-stage root hairs (Supplementary Fig. S9C). In elongating root hairs, the fluorescence was detected at the basal region, but not at the root hair tip (Fig. 5E, Supplementary Fig. S9D, E).

Then the root tips showed the fluorescence as the root hairs reached the mature stage (Supplementary Fig. S9F). Therefore, SRPP may not be necessary for the root hair tips in elongating root hairs, but rather is required for maturating root hairs to strengthen the cell wall under stress conditions such as Pi-deficiency. Lack of SRPP weakened the cell wall and in extreme cases caused cell death of root hairs, an observation that supports the above scenarios (Fig. 2).

SRPP is also expressed in the valve of the fruit, funiculus, seed coat, and embryo (Fig. 1). *srpp-1* produced abnormal dark brown, withered seeds, which contained a high frequency of immature embryos (Fig. 3). The developmental arrest and partial death of *srpp-1* embryos abolished in the complemented lines (Supplementary Fig. S8). Therefore, SRPP is required to protect developing embryos under stress during stages before seed maturation. Furthermore, analysis of hybridization between No-0 and *srpp-1* (Fig. 4) revealed that the expression of SRPP in maternal tissues (valve, funiculus, and seed coat) is necessary for normal formation of seeds.

The cell walls provide a structural framework and prevent overexpansion of cells to maintain cell shapes. Because SRPP contains several positively charged residues such as lysine, and its pI value is 9.21, there is a possibility that SRPP interacts with negatively charged components, including pectins, in the cell wall. Thus, we estimate that SRPP is involved in the regulation of cell wall rigidity. Pectins are rich in the middle lamella, and thought to be involved in the extensibility of the cell wall through the formation a functionally and structurally diverse class of galacturonic acid-rich polysaccharides (Daher and Braybrook 2015, Wolf and Greiner 2012). The actual physiological roles of SRPP, including the above hypothetical properties, remain to be resolved.

In general, the structure and composition of the cell wall are variable between different cell types and tissues. Furthermore, the cell wall structures change dynamically during cell growth and in response to stresses (Fry 2004). Plant cells contain a thin primary cell wall that is extensible and composed of pectin, cellulose, hemicellulose, and a small amount of protein. Secondary cell walls are produced by specialized cell types such as vascular bundles and serve shielding and structural reinforcing roles (Kumar et al. 2016). Cells of root hair and embryo are surrounded by only the primary cell wall. The root hairs and embryos need to maintain higher

activities of water absorption and nutrient uptake compared with the other cells. Therefore, these cells do not form the secondary cell wall. SRPP may play a key role in the cell walls of root hairs and seeds to maintain the specific structure and properties of these walls.

In conclusion, this study has revealed the following three major findings. First, we identified the novel SRPP protein, which is partially homologous to PRPs but does not contain the Pro-rich region. Second, SRPP is expressed specifically in root hairs and fruits and is localized in the cell wall. Third, the loss-of-function of *SRPP* causes an abnormal phenotype in root hairs and seeds. The morphological abnormality of *srpp-1* was found in the cell wall. The defect of cell wall may be a major cause of the phenotype of the *srpp-1* line, in which the cells and tissues are not protected by intact cell walls against stresses resulting in a high frequency of cell death during development. Thus, we estimate that SRPP protects root hairs and seeds from some stresses, such as Pi-deficiency and drought stress. To reveal the biochemical and physiological mechanisms of root hair and seed protection, further studies should be carried out, with priority given to the examination of the biochemical properties of SRPP and its interactions with the plasma membrane and cell wall components.

Materials and Methods

Plant materials and growth conditions

Seeds of *A. thaliana* (strain No-0) and the loss-of-function mutant *srpp-1* (RATM13-5238-1; Supplementary Fig. S4A) were provided by the Riken Bioresource Center (Tsukuba, Japan). The *srpp-1* mutant line was confirmed to be homozygous by genotyping using *SRPP*-specific primers (5'-CACCCGCTGGTTTACCAATCATA-3' and 5'-GCATTTGGTCACTGTCCTTCCTG-3'), and a primer specific to the G-edge of a transposon (5'-TACCTCGGGTTCGAAATCGAT-3'). The seeds were surface-sterilized and sown on sterile gel plates containing half-strength MS salt mixture, 2.5 mM MES-KOH (pH 5.7), 1% (w/v) sucrose, and 1.2% Ina agar (Funakoshi, Tokyo, Japan) (MS plates). Seed specimens were placed in darkness at 4°C for 3 d, and then moved to a growth chamber at 22°C under long-day conditions (light/dark regime of 16 h/8 h, cool-white lamps, 80–110 μmol m^{-2} s^{-1}). A modified

culture medium of Hoagland medium not supplemented with Pi was prepared to evaluate the effect on the plant growth under Pi-deficient conditions.

Construction of transgenic plants

For *SRPP*p::SRPP construction, the region at −1951 to +867 of *SRPP* was amplified from *A. thaliana* (strain, No-0) genomic DNA using KOD FX enzymes (Toyobo, Tokyo, Japan) with the pair of oligonucleotides (Supplementary Table S1). The amplified sequence was inserted into an entry vector using a TOPO cloning reaction kit (Invitrogen, Carlsbad, CA, USA) and then subcloned into a pGWB401 vector (*SRPP*p::SRPP/pGWB401) by LR reaction using Gateway LR Clonase II Enzyme Mix (Invitrogen). For *SRPP*p::GUS construction, the region at –1951 to +21 of *SRPP* in genomic DNA was inserted into the pGWB433 (*SRPP*p::GUS/pGWB433). For SRPP-GFP construction, the region at −1951 to +611 of *SRPP* in genomic DNA was inserted into the pGWB604 vector (*SRPP*p::SRPP-GFP/pGWB604) and pGWB404m vector (*SRPP*p::SRPP-GFP/pGWB404m), which included a sequence of the monomer type GFP (Segami et al. 2014).

The prepared constructs (*SRPP*p::SRPP/pGWB401, *SRPP*p::GUS/pGWB433, *SRPP*p::SRPP-GFP/pGWB604 and *SRPP*p::SRPP-GFP/pGWB404m) were introduced into the *Agrobacterium tumefaciens* strain GV3101::PM90 by electroporation and used to transform *A. thaliana* plants using the floral dip method (Clough and Bent 1998). *SRPP*p::SRPP/pGWB401 and *SRPP*p::SRPP-GFP/pGWB604 were introduced into the non-functional line *srpp-1*. *SRPP*p::GUS/pGWB433 and *SRPP*p::SRPP-GFP/pGWB404m were introduced into No-0. After selection with 10 mg ml^{-1} BASTA or 50 mg ml^{-1} kanamycin, multiple T_2 heterozygous or T_3 homozygous lines were used for each experiment.

RNA extraction and RT-PCR

Total RNA fractions were prepared from 2-week-old plants (shoot and root) and 6-week-old plants (silique) using a QIA shredder and RNeasy Mini kit (Qiagen, Valencia, CA, USA). RNA (0.5 μg) was converted into cDNA using a ReverTra Ace qPCR RT Master Mix with gDNA Remover (Toyobo). The primer sets used for the RT-PCR were ATGGAGTCTTCAAGTCCCCAC (Fw) and

CCGGAAGCATTCTTAGAATCTG (Rv) for *SRPP*, CTGATGTTGCAGCCTTTGCA (Fw) and TTTGCCTTCCATCCCGAA (Rv) for *UBQ10*.

GUS staining

T_3 *SRPP*p::GUS/pGWB433 transformants were assayed for GUS activity. The seedlings, siliques, and seeds were stained with a GUS staining solution containing 0.5 mg ml^{-1} 5-bromo-4-chloro-3-indolyl-β-D-glucuronide, 0.5 mM $K_3Fe(CN)_6$, 0.5 mM $K_4Fe(CN)_6$, and 0.3% (w/v) Triton X-100. Seedlings (1- and 3-week-old) were incubated in the solution at 37°C for 2 and 3 h, respectively. Siliques were cut or the valve was removed, they were infiltrated with the solution under a vacuum for 10 min, and then incubated at 37°C for 24 h. The embryos and seed coats of mature seeds were separated, put into different microtubes, infiltrated with the solution under vacuum for 10 min, and then incubated at 37°C for 24 h.

Observation of GFP signals

Seeds of T_2 lines, which contained the SRPP-GFP fusion protein under the control of the *SRPP* promoter, were grown on MS plates containing kanamycin for 11 d, and then grown on Hoagland plates with or without Pi for 6 d. Observations were collected using an upright FV1000-D confocal laser scanning microscope (Olympus, Tokyo, Japan) (Segami et al. 2014). Excitation wavelength and transmission range for emission were 488 and 500–560 nm, respectively. The images were obtained using Olympus Fluoview software and an UPLSAPO 10× objective lens (Olympus).

Microscopic observations of root hairs and measurements of root hair length

Root hair morphology was observed using an optical microscope BX61 (Olympus) equipped with a CCD camera DP70 (Olympus) and a stereoscope SZ61 (Olympus). Root hair length was measured from photomicrographs. The free software package ImageJ (http://rsbweb.nih.gov/ij/) was used for the measurement of root hair length.

PI staining

We observed root hairs and embryos using an FV1000 confocal laser scanning microscope (Olympus) after staining with PI (0.01 mg ml^{-1}) for 1–2 min. The excitation

wavelength and transmission range for emission were 473 and 617–717 nm, respectively. The Olympus Fluoview software was used to obtain pictures.

Scanning electron microscopy

For SEM observations, seeds or fruits (siliques) were harvested and fixed overnight in formalin-acetic acid-alcohol (4% formalin, 5% acetic acid, and 50% ethanol) at room temperature. The fixed specimens were dehydrated in an ethanol series [50, 60, 70, 80, 90, 95, 99.5, and 100% (v/v); 60 min per step] and stored overnight in 100% (v/v) ethanol at room temperature. The ethanol was replaced with 3-methylbutyl acetate and the samples were dried in a critical-point dryer JCPD-5 (JEOL, Tokyo, Japan), sputter-coated with gold-palladium using an anion sputter device JFC-1100 (JEOL) and examined under an S-3400N SEM (Hitachi, Tokyo, Japan) as previously described (Maeda et al. 2014).

Transmission electron microscopy

Mature seeds of No-0 and *srpp-1* were fixed with 4% paraformaldehyde and 2% glutaraldehyde in 0.05 M cacodylate buffer at pH 7.4. After fixation, the samples were washed three times with 0.05 M cacodylate buffer, and were postfixed with 2% osmium tetroxide (OsO_4) in 0.05 M cacodylate buffer. The samples were dehydrated in graded ethanol solutions (50, 70, 90, and 100%). After these dehydration processes, the samples were dehydrated continuously in 100% ethanol. The samples were infiltrated with propylene oxide (PO) twice and put into a 70:30 mixture of PO and Quetol-651 resin (Nisshin EM, Tokyo, Japan). Then the PO was volatilized from the tubes overnight. The samples were transferred to a fresh 100% resin, and were polymerized at 60°C for 48 h. The polymerized resins were sectioned ultra-thin at 70 nm with a diamond knife using an ultramicrotome (Ultracut UCT; Leica, Vienna, Austria) and the sections were mounted on copper grids. They were stained with 2% uranyl acetate at room temperature for 15 min, and then washed with distilled water followed by secondary-staining with lead stain solution (Sigma-Aldrich, St Louis, MO, USA) at room temperature for 3 min. The grids were observed using a transmission electron microscope JEM-1400Plus (JEOL, Tokyo, Japan) at an acceleration voltage of 80 kV. Digital images (2048×2048 pixels) were taken with a CCD camera (Veleta,

Olympus Soft Imaging Solutions GmbH, Münster, Germany).

Statistical analyses of data

To determine the fresh weights of organs and for quantification of the length of primary roots and root hairs, data from at least three independent experiments were averaged, and the values were subjected to statistical analyses using the Student's *t*-test.

Supplementary data

Supplementary data are available at PCP online

Funding

This work was supported by JSPS KAKENHI grant numbers 26252011 and 26113506 to M.M and by Grant-in-Aid for JSPS Fellows 26002201 to N.T.

Acknowledgments

We are grateful to Mariko Kato (Kyoto University, Japan) for giving us the NR23 line, Yoichiro Fukao and Rie Kurata (Nara Institute for Science and Technology, Japan) for LC-MS analysis, and Yoichi Nakanishi, Miki Kawachi, and Shoji Segami (Nagoya University, Japan) for valuable advice.

References

Boron, A.K., van Orden, J., Markakis, M.N., Mouille, G., Adriaensen, D., Verbelen, J.P. et al. (2014) Proline-rich protein-like PRPL1 controls elongation of root hairs in *Arabidopsis thaliana*. *J. Exp. Bot.* 65: 5485–95.

Clough, S.J. and Bent, A.F. (1998) Floral dip: a simplified method for *Agrobacterium*-mediated transformation of *Arabidopsis thaliana*. *Plant J.* 16: 735–743.

Daher, F.B. and Braybrook, S.A. (2015) How to let go: pectin and plant cell adhesion. *Front. Plant Sci.* 6: 523.

Datta, S., Kim, C.M., Pernas, M., Pires, N.D., Proust, H., Tam, T. et al. (2011) Root hairs: development, growth and evolution at the plant–soil interface. *Plant Soil.* 346: 1–14.

Dolan, L. (2001) The role of ethylene in root hair growth in *Arabidopsis*. *J. Plant Nutr. Soil Sci.* 164: 141–145.

Emons, A.M.C., and Ketelaar, T. (2009) Root hairs. *Plant Cell Monographs. Vol. 12*. Berlin: Springer-Verlag.

Foehse, D. and Jungk, A. (1983) Influence of phosphate and nitrate supply on root hair formation of rape, spinach and tomato plants. *Plant Soil.* 74: 359–368.

Francoz, E., Ranocha, P., Burlat, V. and Dunand, C. (2015) *Arabidopsis* seed mucilage secretary cells: regulation and dynamics. *Trends Plant Sci.* 20: 515–524.

Fry, S.C. (2004) Primary cell wall metabolism: tracking the careers of wall polymers in living plant cells. *New Phytol.* 161: 641–675.

Fukao Y, Ferjani, A., Tomioka, R., Nagasaki, N., Kurata, R., Nishimori, Y. et al. (2011) The iTRAQ analysis reveals mechanisms of growth defects due to excess zinc in *Arabidopsis thaliana*. *Plant Physiol.* 155:1893–1907.

Gahoonia, T.S., Nielsen, N.E., Joshi, P.A. and Jahoor, A. (2001) A root hairless barley mutant for elucidating genetic of root hairs and phosphorus uptake. *Plant Soil.* 235, 211–219.

Gilroy, S. and Jones, D.L. (2000) Through form to function: root hair development and nutrient uptake. *Trends Plant Sci.* 5: 56–60.

Grebe, M. (2012) The patterning of epidermal hairs in *Arabidopsis* – updated. *Curr. Opin. Plant Biol.* 15: 31–37.

Grierson, C., Nielsen, E., Ketenlaar, T. and Schiefelbein, J. (2014) Root hairs. The Arabidopsis Book, e0172.

Haughn, G. and Chaudhury, A. (2005) Genetic analysis of seed coat development in *Arabidopsis*. *Trends Plant Sci.* 10: 472–777.

Ide, Y., Nagasaki, N., Tomioka, R., Suito, M., Kamiya, T. and Maeshima, M. (2007) Molecular properties of novel, hydrophilic cation-binding proteins associated with the plasma membrane. *J. Exp. Bot.* 58: 1173–1183.

Kato, M., Nagasaki-Takeuchi, N., Ide, Y. and Maeshima, M. (2010) An *Arabidopsis* hydrophilic Ca^{2+}-binding protein with a PEVK-rich domain, PCaP2, is associated with the plasma membrane and interacts with calmodulin and phosphatidylinositol phosphates. *Plant Cell Physiol*. 51: 366–379.

Kato, M., Aoyama, T. and Maeshima M. (2013) The Ca^{2+}-binding protein PCaP2 located on the plasma membrane is involved in root hair development as a possible signal transducer. *Plant J.* 74: 690–700.

Kumar, M., Campbell, L. and Turner, S. (2016) Secondary cell walls: biosynthesis and manipulation. *J. Exp. Bot.* 67: 515–531.

Kwasniewski, M., Nowakowska, U., Szumera, J., Chwialkowska, K. and Szarejko, I. (2013) iRoot hair: A comprehensive root hair genomics database. *Plant Physiol.* 161: 28–35.

Libault, M., Brechenmacher, L., Cheng, J., Xu, D. and Stacey, G. (2010) Root hair systems biology. *Trend Plant Sci.* 15: 641–650.

Ma, Z., Bielenberg, D.G., Brown, K.M. and Lynch, J.P. (2001) Regulation of root hair density by phosphorus availability in *Arabidopsis thaliana*. *Plant Cell Env.* 24: 459–467.

Maeda, S., Gunji, S., Hanai, K., Hirano, T., Kazama, Y., Ohbayashi, I. et al. (2014) The conflict between cell proliferation and expansion primarily affects stem organogenesis in *Arabidopsis*. *Plant Cell Physiol.* 55: 1994–2007.

Pitts, R.J., Cernac, A. and Estelle, M. (1998) Auxin and ethylene promote root hair elongation in *Arabidopsis*. *Plant J.* 16: 553–560.

Rajjou, L. and Debeaujon, I. (2008) Seed longevity: survival and maintenance of high germination ability of dry seeds. *C. R. Biologies* 331: 796–805.

Segami, S., Makino, S., Miyake, A., Asaoka, M. and Maeshima, M. (2014) Dynamics

of vacuoles and H^+-pyrophosphatase visualized by monomeric green fluorescent protein in *Arabidopsis*: artifactual bulbs and native intravacuolar spherical structures. *Plant Cell* 26: 3416–3434.

Tanaka, N., Kato, M., Tomioka, R., Kurata, R., Fukao, Y., Aoyama, T. et al. (2014) Characteristics of a root hair-less line of *Arabidopsis thaliana* under physiological stresses. *J. Exp. Bot.* 65: 1497–1512.

Wolf, S. and Greiner, S. (2012) Growth control by cell wall pectins. *Protoplasma* 249: S169–S175.

Won, S.K., Lee, Y.J., Lee, H.Y., Heo, Y.K., Cho, M. and Cho, H.T. (2009) *Cis*-element- and transcriptome-based screening of root hair-specific genes and their functional characterization in *Arabidopsis*. *Plant Physiol.* 150: 1459–1473.

Figure legends

Fig. 1 SRPP is expressed predominantly in roots and siliques. (A) RNA fractions were prepared from 2-week-old plants (shoot and root) and 6-week-old plants (silique) of No-0 and *srpp-1*. RNA was converted into cDNA and subjected to RT-PCR. (*B*–*D*) *SRPP*p::GUS lines (T_3 homozygous lines) were grown on Hoagland medium containing 0 (B, right panel) or 280 μM Pi (B, left panel; C and D) for 1 (B, D) or 3 weeks (C) and subjected to GUS staining. Arrows indicate the cell line of the root hair (D). (*E*–*G*) Siliques (E and F) at different stages of development (a–d) and seeds (G) of various stages were observed. Enlarged pictures are shown in right panels (a–d). (G) Seeds were cut and stained for GUS to visualize the embryo (left, immature stage), then the embryo was isolated (middle, mature stage), and the seed coat was separated (right, mature stage).

Fig. 2 Root hairs and primary roots of *srpp-1* are short and die under Pi-deficient conditions. No-0 and *srpp-1* were grown on Hoagland medium containing 0 or 280 μM Pi. (A) Each of the five seedlings grown for 14 d were used to measure root hair length. Mature root hairs at the region around 3–7 mm from the root tip were measured. (B) Four-week-old seedlings grown without Pi were subjected to measurements of primary root length. Error bars show SDs; $N \geq 40$ (*A*), $N = 50$ (*B*). Asterisks indicate significant differences at $^{***}P < 0.005$ compared with No-0 (Student's *t*-test). (C) In 16-d-old seedlings grown without Pi, typical root hairs around 1.5 cm from the root tip were observed. Scale bars, 200 μm. (D and E) No-0 and *srpp-1* were grown on the medium containing 280 (D) or 0 μM Pi (E). Roots of 8-d-old seedlings were stained with PI, and then observed by CLSM. Scale bars, 200 μm.

Fig. 3 Seeds of *srpp-1* are withered and embryo development is arrested. (A)

Typical seeds from No-0 and *srpp-1* were observed using a stereoscope. (B) Typical mature siliques and seeds were observed using a scanning electron microscope. (C) Mature seeds were soaked in water for 1 h, and then the embryos was separated from the seed coats and observed. Scale bars, 200 μm. (D) Embryos collected from mature seeds were stained with 10 mg μl^{-1} propidium iodide for 1–2 min, and then observed by CLSM. Scale bars, 100 μm.

Fig. 4 Crossing analysis between No-0 and *srpp-1*. The flowers of 6-week-old seedlings were used for hybridization. Seeds were harvested from matured and dried siliques. (A) Seeds from each silique were grown separately for 3 weeks and typical plates were photographed. (B) The averages of germination rate per silique are shown. Error bars show SDs; $N \geq 8$. Asterisks indicate significant differences at $^{***}P < 0.005$.

Fig. 5 Cell-wall localization of SRPP and abnormality of the cell wall of *srpp-1*. (A–F) SRPP-GFP lines grown for 11 d were transplanted to Hoagland plates without Pi and cultivated for 6 d. Root hair cells were observed by CLSM. (A and B) Untreated root hair cells. (C–F) Root hair cells after plasmolysis by 20% (w/v) sucrose for 10 min. (B, D and F) Merged images of GFP (green) and differential interference contrast images. (E) Arrow heads show the basal region of the root hair (insertion, a contrasted monochrome image). (G–K) The cell walls in *srpp-1* seeds show irregular morphology. Thin sections prepared from embryos of No-0 (G and I) and *srpp-1* (H and J) at the mature stage were observed by TEM. The contact point of three cells (blue arrowhead) is marked. (K) Cell wall thickness in the images was measured. Error bars show the maximum and minimum values, boxes show the upper and lower quartiles, and lines in the boxes indicate the median.

Fig. 1 Tanaka et al.

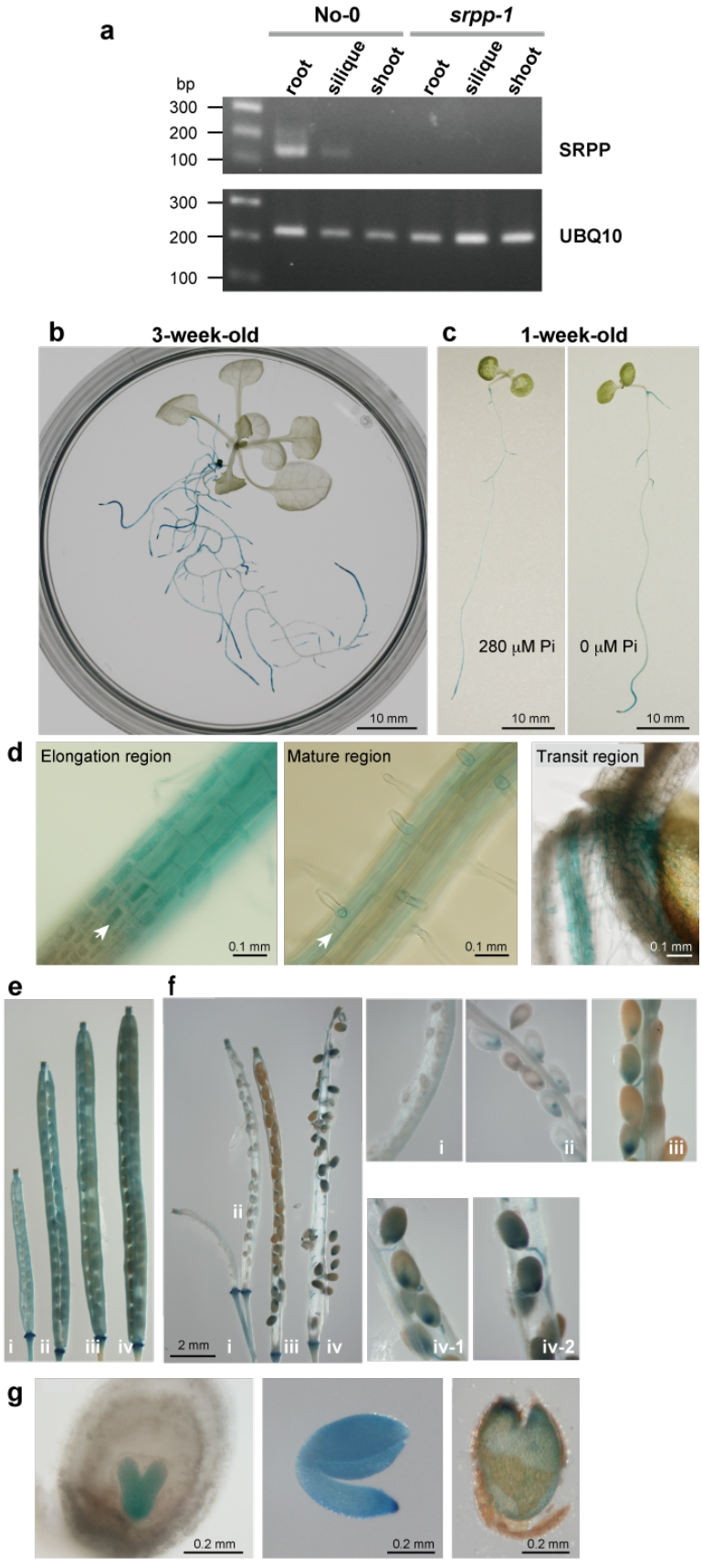

Fig. 2 Tanaka et al.

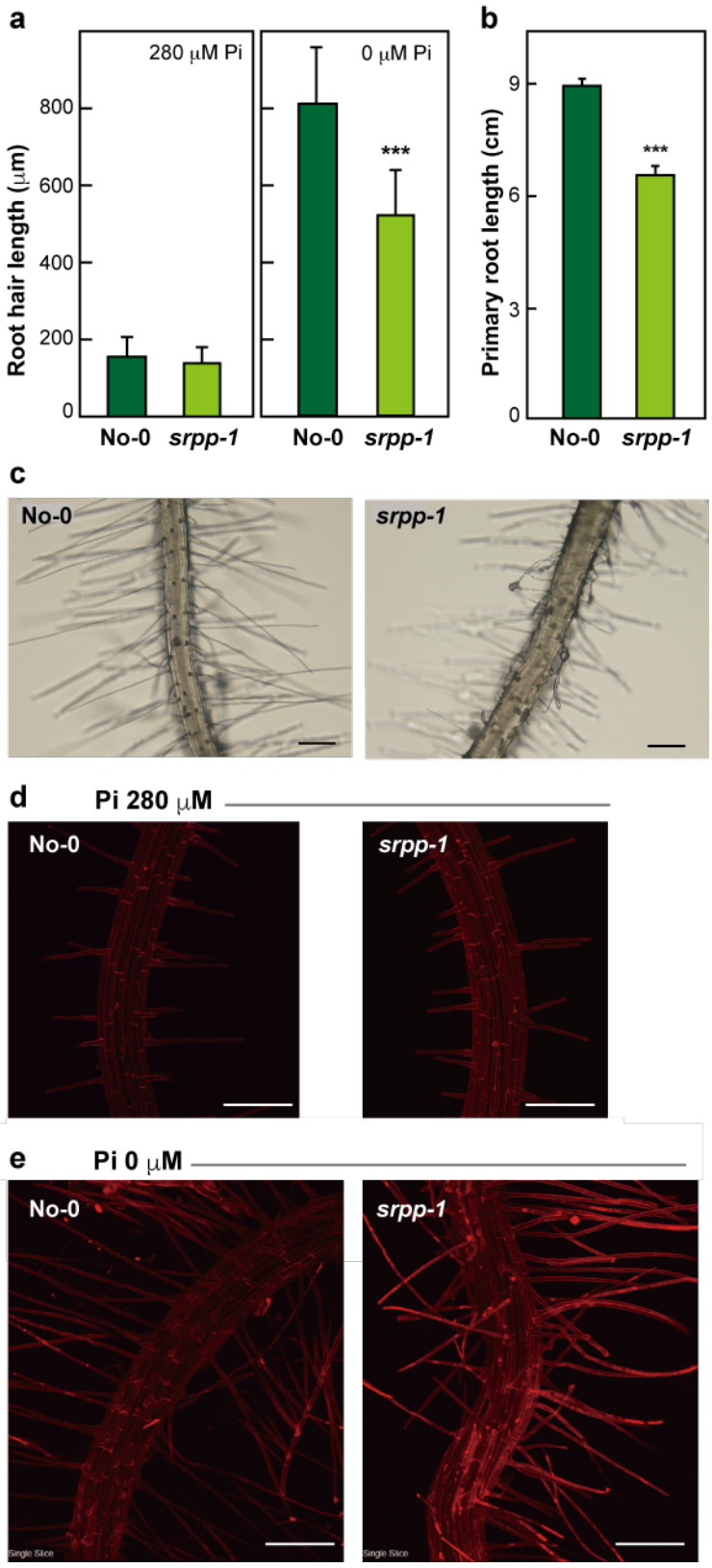

Fig. 3 (Tanaka et al.)

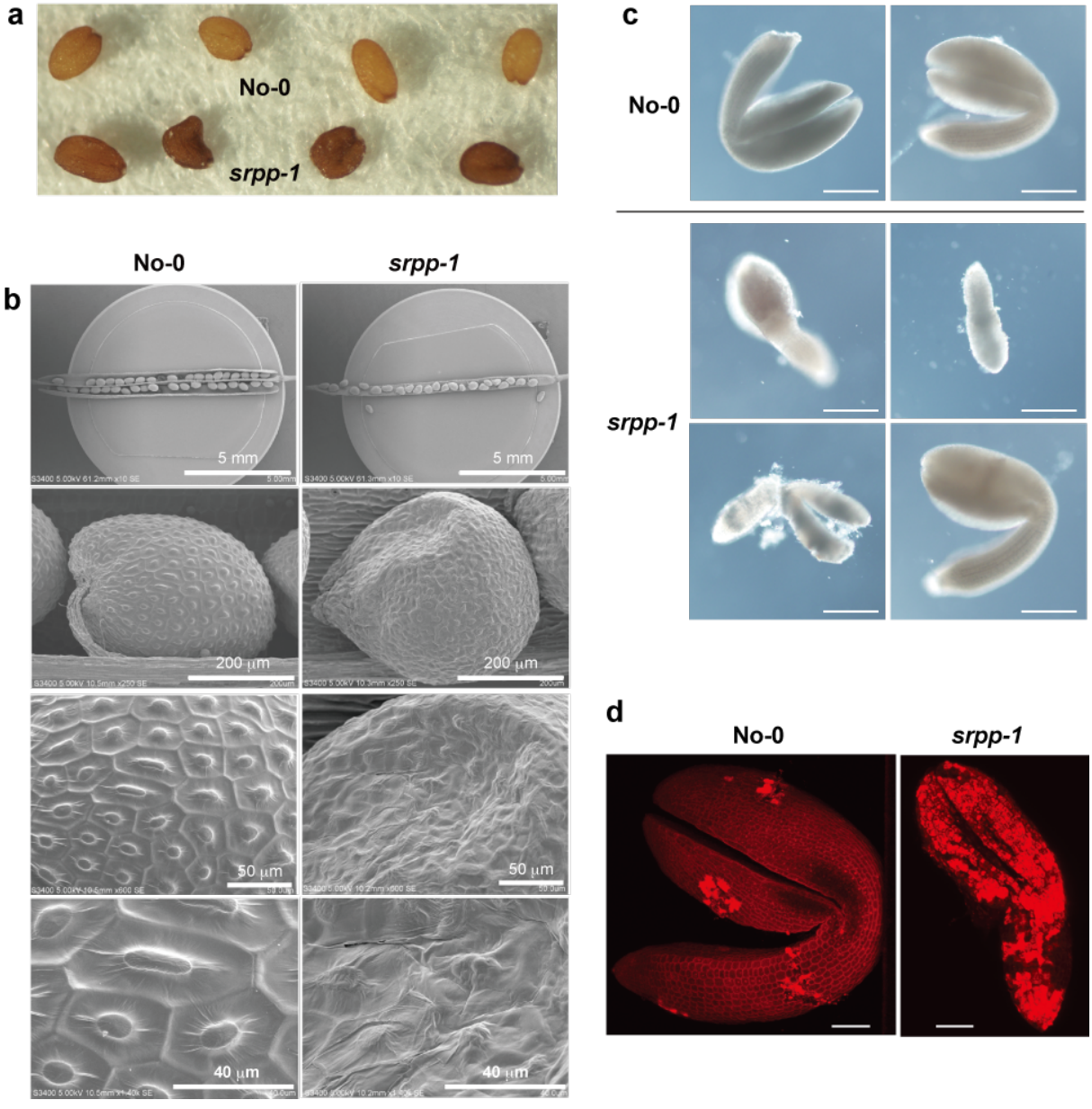

Fig. 4 (Tanaka et al.)

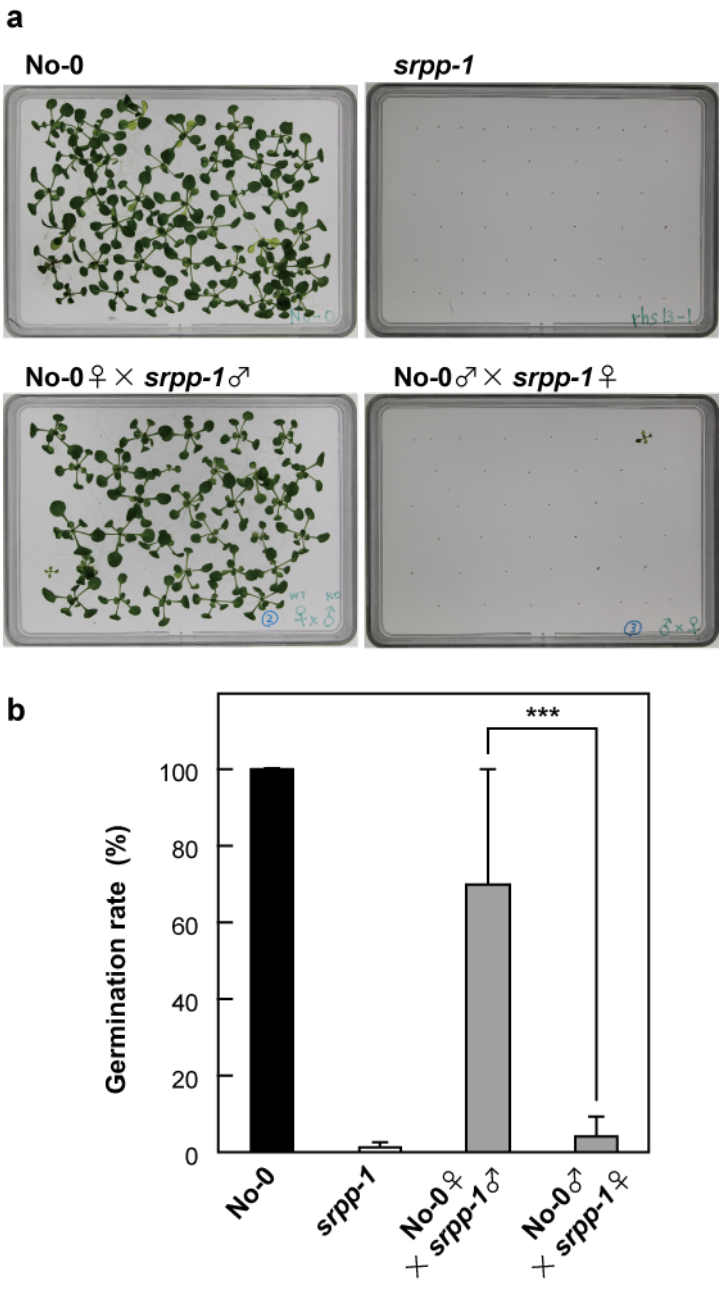

Fig. 5 (Tanaka et al.)